Progressive Spinal Axonal Degeneration and Slowness in ALS2-Deficient Mice

Koji Yamanaka, MD, PhD, Timothy M. Miller, MD, PhD, Melissa McAlonis-Downes, MS, Seung Joo Chun, and Don W. Cleveland, PhD

Objective: Homozygous mutation in the *ALS2* gene and the resulting loss of the guanine exchange factor activity of the ALS2 protein is causative for autosomal recessive early-onset motor neuron disease that is thought to predominantly affect upper motor neurons. The goal of this study was to elucidate how the motor system is affected by the deletion of ALS2.
Methods: ALS2-deficient mice were generated by gene targeting. Motor function and upper and lower motor neuron pathology were examined in ALS2-deficient mice and in mutant superoxide dismutase 1 (SOD1) mice that develop ALS-like disease from expression of an ALS-linked mutation in SOD1.
Results: ALS2-deficient mice demonstrated progressive axonal degeneration in the lateral spinal cord that is also prominent in mutant SOD1 mice. Despite the vulnerability of these spinal axons, lower motor neurons in ALS2-deficient mice were preserved. Behavioral studies demonstrated slowed movement without muscle weakness in $ALS2^{-/-}$ mice, consistent with upper motor neuron defects that lead to spasticity in humans.
Interpretation: The combined evidence from mice and humans shows that deficiency in ALS2 causes an upper motor neuron disease that in humans closely resembles a severe form of hereditary spastic paralysis, and that is quite distinct from amyotrophic lateral sclerosis.

Ann Neurol 2006;60:95–104

Amyotrophic lateral sclerosis (ALS) is a progressive neurodegenerative disease caused by a preferential loss of motor neurons, resulting in progressive weakness of skeletal muscles, atrophy, and death due to respiratory muscle paralysis generally 2 to 5 years after the onset of the disease. The pathology of ALS is characterized by a loss of upper and lower motor neurons and degeneration of pyramidal tracts. Approximately 10% of ALS is inherited. Dominant mutations in Cu/Zn superoxide dismutase 1 (SOD1) have been identified as the most frequent cause of inherited ALS.[1,2]

Homozygous mutation of *ALS2,* initially proposed as a second ALS-related gene,[3–7] is causative for autosomal recessive early-onset motor neuron disease (ALS2),[6–8] a juvenile form of primary lateral sclerosis,[7] and infantile ascending hereditary spastic paralysis.[9–11] Recessive *ALS2* mutations initially were identified in a Tunisian family[6–8] (carrying a frameshift mutation at amino acid 46 of the corresponding ALS2 polypeptide and developing progressive spasticity in all limbs between 3 and 10 years of age), in a Kuwaiti family[6,12] (carrying a frameshift mutation at amino acid 475 of the *ALS2* gene and presenting with infantile-onset [1–2 years old] spastic paralysis without lower motor neuron involvement), and in a Saudi Arabian family[7,13] (carrying a frameshift mutation in ALS2 at amino acid 623 and being diagnosed as juvenile primary lateral sclerosis with infantile-onset [1–2 years old] and preserved lower motor neurons). After these reports, eight additional *ALS2* disease-causing mutations have been identified, all of which have caused infantile-onset, severe spastic paralysis.[9–11,14,15] Inspection of all reported patients with ALS2 mutations (Table) shows that all but one family developed infantile-onset (before 2 years) spastic paralysis with a predominantly upper motor neuron (UMN) defect, although lower motor neurons have been reported to be affected in a minority of ALS2 patients.[8,14] No autopsy report has yet been published to confirm these findings.

The ALS2 protein (also referred as alsin) consists of 1,657 amino acids with 3 putative guanine exchange factor (GEF) domains (Fig 1A). In the nervous system, it is preferentially associated with the cytoplasmic face of endosomal membranes,[16–18] an association that requires its amino-terminal regulator of chromatin condensation (RCC1)–like GEF domain.[16] ALS2 has been

From the Ludwig Institute for Cancer Research and Department of Medicine and Neurosciences, University of California, San Diego, La Jolla, CA.

Received Dec 29, 2005, and in revised form Apr 7, 2006. Accepted for publication Apr 15, 2006.

Published online June 26, 2006 in Wiley InterScience (www.interscience.wiley.com). DOI: 10.1002/ana.20888

Address correspondence to Dr Yamanaka, Ludwig Institute for Cancer Research, University of California, San Diego, 9500 Gilman Drive, CMM-East 3080, La Jolla, CA 92093-0670.
E-mail: kyamanaka@ucsd.edu

Table. Infantile Disease Onset in Most Patients with ALS2 Mutations

Mutation	A46fs	C156Y	T185fs	I336fs	T475fs	V491fs	L623fs	N846fs	R998st	M1207st	V1574fs
Location of mutation, exon	3	4	4	4	5	6	9	13	18	22	32
Mutant ALS2 product, amino acid	49	1657	188	339	545	492	645	857	997	1206	1616
Onset, yr	3–10[a]	1	2	1.5	1.2	1.5	1–2	1.4	1	1	1.5
Loss of walking, yr	12–50[a]	<3–6	<12	4	NA	4	NA	5	NA	NA	+[b]
Bulbar symptom, yr	+[b]	12–16	15	13	4	8	2–10	12	3	13	<12
Upper/Lower motor symptom	U/L[c]	U	U/L	U	U	U	U	U	U	U	U
References	6–8	15	14	9, 30	6, 12	9, 30	7,13	9, 30	11	9,30	10

[a]Not all cases are genetically diagnosed.
[b]Observed, but age was not reported.
[c]Fifty percent of cases show lower motor neuron symptoms.
fs = frameshift mutation; st = (stop) nonsense mutation; NA = never able to walk.

shown to act in vitro as a GEF for two small GTPases, Rab5[17,18] and Rac1,[18–20] that are known to be involved in endosomal trafficking and actin cytoskeleton remodeling, respectively. A feature common to all disease-causing *ALS2* mutations is a loss of protein stability, suggesting that a loss of ALS2 is causative for this early-onset motor neuron disease.[16] A smaller isoform of 396 amino acids in humans[6,7] (or 928 amino acids in mice[21]) has been proposed from the presence of an alternatively spliced messenger RNA that is most prominent outside the nervous system,[6,21] but there is no evidence for accumulation of the predicted polypeptide.

Deficiency of ALS2 in mice has been reported to show mild age-dependent motor coordination and learning impairment, a higher level of anxiety response, and increased susceptibility of oxidative stress without obvious neuropathology,[22] or slowly progressive loss of cerebellar Purkinje cells and modest denervation and reinnervation of lower motor neurons without manifesting motor impairment.[21] Whether the UMN system, the lesion most relevant to *ALS2*-mutated patients, is affected in ALS2-deficient mice has not been examined. To elucidate how the motor system is affected by the deletion of ALS2, we have generated $ALS2^{-/-}$ mice. By evaluating running speed, analysis of these mice showed a moderate impairment in coordination and slowness without muscle weakness. Slowness of movements is a well-recognized clinical sign of a UMN defect observed in human patients including ALS.[23–25] Absence of ALS2 also resulted in progressive degeneration of spinal cord axons predominantly in the lateral columns. These same axons are also shown to be severely damaged in mutant SOD1 transgenic mice,[26] a mouse model for inherited ALS. The lower motor neurons, which are severely affected in SOD1 mice, are completely preserved even in aged $ALS2^{-/-}$ mice. The pathology and phenotype of $ALS2^{-/-}$ mice is similar to that of mouse models of hereditary spastic paralysis.[27,28] Combined with the recognition that disease initiates before 2 years of age in almost all ALS2 patients, it is clear that in both mice and humans, loss of ALS2 causes UMN disease that is distinct from ALS.

Materials and Methods

Generation of ALS2-Deficient Mice

A BAC (Bacterial Artificial Chromosome) clone containing mouse *ALS2* gene (RPCI-22 16O13) isogenic to TC1 embryonic stem (ES) cells (129SvEvTac) was identified using high-density membrane available from BACPAC Resource Center at the Children's Hospital Oakland Research Institute (Oakland, CA; http://bacpac.chori.org). For ALS2 targeting vector, 1.5kb *Dra*I-*Bgl*II and 9.7kb *Eco*RI restricted genomic DNA fragments homologous to mouse *ALS2* gene as 5′ and 3′ fragments, respectively, were cloned together with PGK-neo and HSV-TK cassette for selection (see Fig 1B). Targeting the *ALS2* locus resulted in a truncated ALS2 polypeptide (174 amino acids) due to an insertion of a stop codon. The linearized vector was electroporated into TC1 ES cells, and cells were selected by 250μg/ml G418 and 2μM gancyclovir. Correctly targeted clones by the homologous recombination were confirmed by Southern blot using a probe located outside the homology region (see Figs 1B, C). Two targeted clones were injected into C57/B6 blastocysts to generate chimeras, which were subsequently used as founders to breed F1 $ALS2^{+/-}$ mice. The F1 $ALS2^{+/-}$ mice were interbred to obtain wild-type, heterozygous, and homozygous littermates (F2; mixed 129SvEvTac/C57BL6 genetic background), which were used for behavioral and pathological

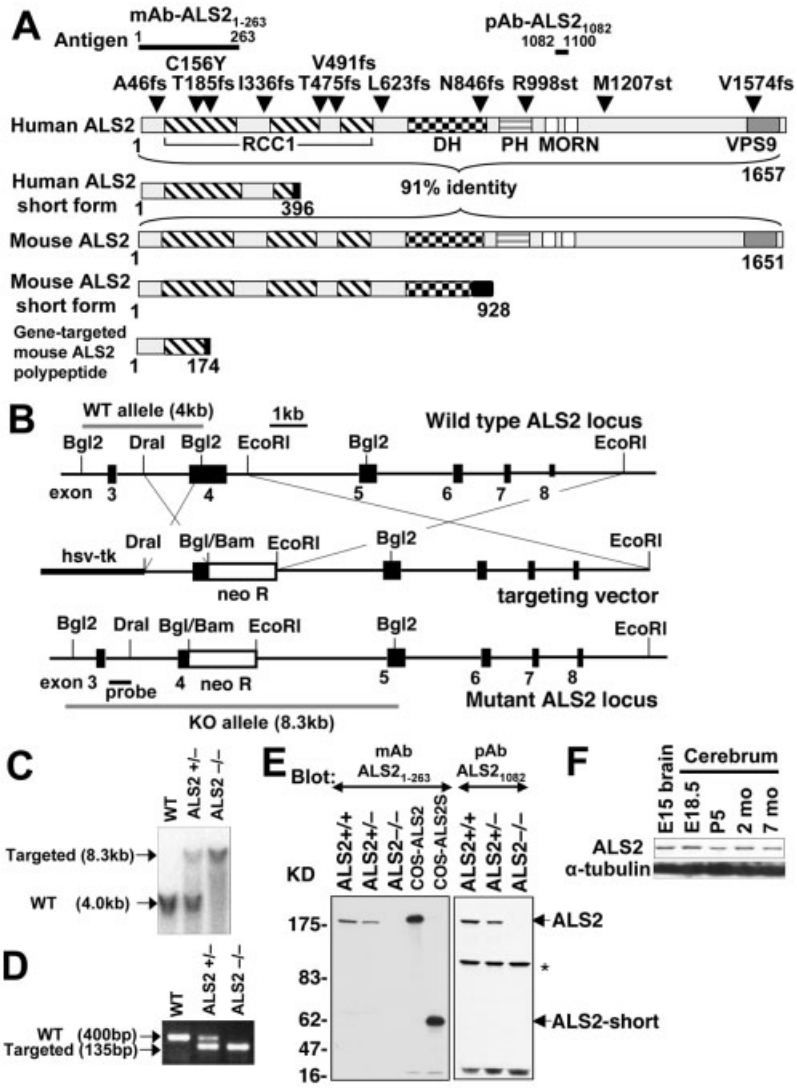

Fig 1. Construction of ALS2$^{-/-}$ mice. (A) Domain structure of human and mouse ALS2 protein, their proposed short forms, and mouse ALS2 polypeptide produced after gene targeting. Known ALS2 disease-causing mutations are also depicted. Insertion of neomycin-resistant gene into the mouse ALS2 *gene produces a translation product of only 171 intact amino acids followed by 3 unique residues and a premature stop codon at amino acid 175. New amino acid residues due to the alternative splicing or frame-shift are shown* (black box). *Antigens for generation of ALS2 antibodies are shown at the top. (B) Schematic diagram of ALS2 gene targeting. A map of wild-type (WT) ALS2 locus, the targeting vector, and the ALS2 mutant allele is shown. The targeting vector was designed to replace most of exon 4 and subsequent intron with neomycin-resistant gene (neo R), resulting in an insertion of a stop codon. (C, D) Analysis of genomic DNA from WT, heterozygous (ALS2$^{+/-}$), and ALS2 knock-out (ALS2$^{-/-}$) mice by Southern blot (C) and polymerase chain reaction (PCR) (D). The* Bgl*II-restricted fragments detected for WT (4kb) and targeted (8.3kb) ALS2 alleles with probe are indicated (C). WT and targeted PCR products are shown (D). (E) Brain extracts (70μg) from WT (ALS2$^{+/+}$), heterozygous (ALS2$^{+/-}$), and ALS2 knock-out (ALS2$^{-/-}$) mice together with COS cells lysates (2μg) transfected with WT ALS2 (COS-ALS2) or ALS2 short form (COS-ALS2S) expression plasmids were analyzed by immunoblots using anti-ALS2 antibody as indicated.* Asterisk *indicates nonspecific band. (F) Extracts of brain and cerebrum (40μg) from indicated age of WT mice were immunoblotted with anti-ALS2 and anti–α-tubulin antibody. DH = dbl homology; MORN = Membrane Occupation and Recognition Nexus motif; PH = pleckstrin homology domain related to a guanine exchange factor (GEF) for the Rho family; RCC1 = regulator of chromatin condensation (RCC1)–like domain, a GEF for the small G protein Ran; VPS9 = vacuolar protein sorting 9 domain, a GEF for the GTPase Rab5.*

analysis. Genotyping was performed by polymerase chain reaction using three primers; the targeted fragment (135bp) was amplified by 5′ALS2 primer (GAACACACACTGGCATTGTCACTCAGCAG) and 3′neo primer (ATGGCTTCTGAGGCGGAAACAACCAGC), and wild-type fragment (400bp) by 5′ALS2 primer and 3′ALS2 primer (GCAATGGCTGTCCGATATTATCACATGGTC). SOD1^{G85R} mice were described previously.[26]

Antibodies

For generating a monoclonal antibody (mAb-ALS2$_{1\text{-}263}$), histidine-tagged ALS2 polypeptide (amino acids 1–617) was used as an antigen.[16] Hybridomas made by fusion of spleen and myeloma cells were selected, cloned, and screened by enzyme-linked immunosorbent assay. Ascites fluid was generated by intraperitoneal injection of the hybridoma into mice. The epitope was determined by immunoblot using amino-terminally truncated ALS2 expression constructs.[16] A polyclonal antibody (pAb-ALS2$_{1082}$)[16] and anti-α-tubulin antibody (Sigma, St. Louis, MO) were described previously.

Plasmids and Transfection

Expression vectors, pCIneoFL-ALS2 (wild type), ALS2 short form, were described previously.[16] COS cells were transfected transiently with Fugene 6 (Roche Diagnostics, Indianapolis, IN) according to the manufacturer's instructions.

Tissue Extract and Immunoblots

Transfected COS cells were lysed with lysis buffer (1% Triton X-100 [Sigma], 50mM tris(hydroxymethyl)aminomethane-HCl pH 7.5, 150mM NaCl) and protease inhibitor cocktail (1μg/ml aprotinin, 1μg/ml leupeptin, and 1mM phenylmethyl sulfonyl fluoride). Mouse tissues were also homogenized in lysis buffer. After centrifugation, the clarified supernatant was analyzed by immunoblot.

Behavioral Assay

Grip strength was measured using a Grip Strength Meter (Columbus Instruments, Columbus, OH). Mice were allowed to grip a triangular bar only with hind limbs, followed by pulling the mice until they released; five force measurements were recorded in each separate trial. For rotarod analysis, mice were placed on the rotating rods automatically accelerating from 0 to 40*g* for 4 minutes (Rotor-Rod System, San Diego Instruments, San Diego, CA). The latency of time to fall from the rotating rod was recorded. Mice were tested for three trials. For running speed, a bike computer (Cordless 7; CAT EYE, Osaka, Japan) was attached to the running wheel (13cm diameter, Activity Wheel; Lafayette Instrument, Lafayette, IN) to measure the distance and average speed of running by detecting the revolution of the wheel with digital magnetic counters. Activity of the mice was restricted on the wheel during three consecutive measurements (5 minutes per trial) in a dark room. All behavioral studies were performed with the genotype unknown to the examiner.

Tissue Preparation and Morphological Analysis

Mice were perfused transcardially with 4% paraformaldehyde in 0.1M phosphate buffer, pH 7.4. Brain and spinal cord tissues were embedded with paraffin and stained with Luxol fast blue. Spinal cords and L5 roots transversely sectioned into 5mm blocks were treated with 2% osmium tetroxide in 0.05M cacodylate buffer, washed, dehydrated, and embedded with Epon (Electron Microscopy Sciences, Hatfield, PA). One-micrometer cross sections were stained with 1% toluidine blue. Axonal diameters of L5 roots were measured by Bioquant software (BIOQUANT Image Analysis Corporation, Nashville, TN). Entire roots were imaged, imaging thresholds were selected individually, and the cross-sectional area of each axon was calculated and reported as a diameter of a circle of equivalent area. Axon diameters were grouped into 0.5μm bins.

For counting degenerating axons in the spinal cord, the degenerated axons were determined by axonal swelling, loss of myelin structure, or abnormal toluidine blue–positive accumulations within axoplasm.

For counting Purkinje cells, tissues were fixed in 4% paraformaldehyde in 0.1M phosphate buffer, pH 7.4, frozen, sectioned (30μm), and stained with cresyl violet. Purkinje cells were counted in every 25th sagittal section through entire cerebellum as described elsewhere.[29] The number of degenerated axons in the lateral column and dorsal column of spinal cord cross sections and number of the Purkinje cells in cerebellar sagittal sections were counted under bright-field microscope by an experimenter blinded to the genotype.

Results

Generation of ALS2-Deficient Mice

To generate an ALS2-deficient mouse model, we used homologous recombination in mouse ES cells to disrupt the mouse *ALS2* gene. A targeting construct was designed to replace 1.5kb of the *ALS2* gene containing exon 4 and a portion of intron 4 with a neomycin-resistant gene. This yielded a gene with a premature translation terminator at amino acid 175 of both the 1,651-amino acid full-length ALS2 product and the proposed 928-amino acid shorter isoform (see Figs 1A, B). Four targeted ES clones were identified, two of which were used to generate *ALS2*$^{+/-}$ mice. Homologous recombination was confirmed by genomic DNA blotting and polymerase chain reaction (see Figs 1C, D). Immunoblotting of brain lysates with two independent ALS2 antibodies showed no detectable full-length ALS2 in extracts from *ALS2*$^{-/-}$ mice, confirming the gene disruption of *ALS2* (see Fig 1E). Moreover, neither of the proposed ALS2 short forms, which should migrate at either approximately 60KDa[16] or approximately 100 KDa,[21] could be detected using ALS2$_{1\text{-}263}$ antibody, even in wild-type mice (see Fig 1E).

Because almost all *ALS2*-mutated patients present with infantile disease onset (see the Table) and ALS2 is known to be expressed at highest levels in the brain,[16,17] we initially examined whether expression level of ALS2 was altered during development. The expression level of ALS2 in brain was at a constant level from the embryonic to the adult stage (see Fig 1F).

ALS2-Deficient Mice Showed Motor Impairment in Coordination and Slowness

Interbreeding of ALS2$^{+/-}$ mice was used to produce ALS2 null progeny. *ALS2*$^{-/-}$ mice were born in the expected Mendelian ratio, developed normally, and generally indistinguishable from wild-type littermates. To examine the potential motor impairment of

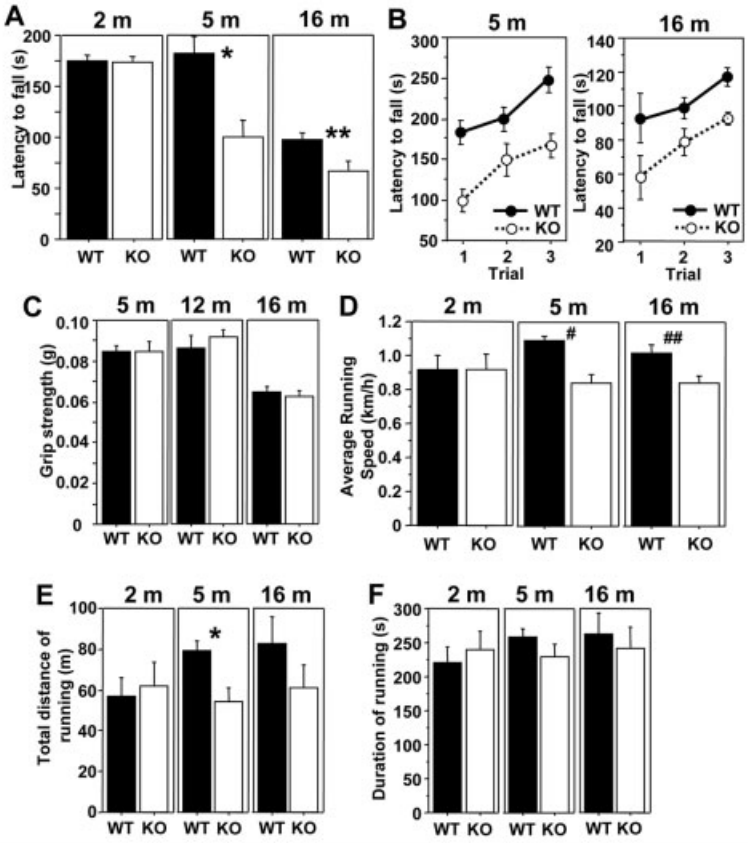

*Fig 2. Deficient motor coordination and slowness of movement in ALS2$^{-/-}$ mice. (A, B) Rotarod analysis of ALS2$^{-/-}$ (knock-out [KO]) and wild-type (WT) mice. (A) The mean latency to fall from the rotating rod at 2 (n = 4), 5 (n = 7), and 16 (n = 4) months is shown. *p < 0.01; **p < 0.03 (unpaired* t *test). (B) The mean holding time of the mice on the rotating rod at 5 (left; n = 7) and 16 months old (right; n = 4) is shown with three sequential trials. Repeated-measures analysis of variance confirmed a statistically significant difference between genotypes at 5 (*p < 0.005*) and 16 months (*p < 0.001*). (C) Preserved grip strength in ALS2$^{-/-}$ mice. Averaged grip strength of ALS2$^{-/-}$ (KO) and WT mice (n = 5 each) at indicated age is plotted. (D) Running speed. The average running speed of ALS2$^{-/-}$ and WT mice at 2 (n = 3), 5 (n = 6), and 16 (n = 4) months old is shown. #p < 0.001; ##p < 0.02 (unpaired* t *test). (E) Total distance of running. The average total distance of run measured simultaneously in (D) is plotted. *p < 0.01 (unpaired* t *test). (F) Duration of running measured simultaneously with running speed in (D).* Error bars *denote standard error.*

ALS2$^{-/-}$ mice, we measured rotarod, grip strength, and running speed. As early as 5 months, ALS2$^{-/-}$ mice showed a shorter latency to fall from the rotating rod compared with wild-type littermates (wild type: 182.3 ± 16.4 seconds; ALS2$^{-/-}$: 100.5 ± 16.9 seconds; $p < 0.01$; n = 7; Fig 2A). The latency was further shortened at 16 months of age (wild type: 97.0 ± 6.9 seconds; ALS2$^{-/-}$: 67.0 ± 9.1 seconds; $p < 0.03$; n = 4; see Fig 2A). All mice showed comparable learning ability as measured by an increasing latency to fall during repeated trials (see Fig 2B). Grip strength of hind limbs showed no difference between wild-type and ALS$^{-/-}$ mice at 5, 12, or 16 months (see Fig 2C).

To further examine whether slowness of movement is associated with a motor coordination decline in ALS2$^{-/-}$ mice, we measured the voluntary running speed of mice using a running wheel equipped with a computer that allowed measurement of running speed, duration of running, and total distance of run. No difference was seen between genotypes at 2 months old (see Fig 2D). By 5 months, average running speed was reduced by approximately 20% in ALS2$^{-/-}$ mice (wild type: 1.094 ± 0.025km/hr; ALS2$^{-/-}$: 0.844 ± 0.051km/hr; $p < 0.001$; n = 7), as well as 16 months of age (wild type: 1.014 ± 0.051km/hr; ALS2$^{-/-}$: 0.84 ± 0.043km/hr; $p < 0.02$; n = 4) (see Fig 2D). The total distance of running was decreased in ALS2$^{-/-}$ mice at 5 and 16 months of age, consistent with the decreased running speed (see Fig 2E). There was no significant difference in duration of running between genotypes (see Fig 2F). Moreover, there was no statistical difference in body weight of the mice used for behavioral studies between genotypes (data not shown).

Preservation of Lower Motor Neurons and Cerebellum in ALS2-Deficient Mice

Because a minority of *ALS2*-mutated patients have been shown to develop lower motor neuron defects (ie, patients in 2[8,14] of 11 reported affected families; see the Table), we examined whether lower motor neurons were affected in $ALS2^{-/-}$ mice. There were no degenerative changes in the axons of L5 motor roots (Figs 3A–D). Aged $ALS2^{-/-}$ mice (16 months) had slightly fewer large caliber axons compared with wild-type littermates; however, a trend of loss of a few motor axons did not reach statistical significance between genotypes (wild type: 958 ± 28; $ALS2^{-/-}$: 866 ± 46; n = 4; $p = 0.13$, unpaired t test) (see Figs 3C, D). Moreover, there were no detectable abnormalities in lumbar motor neurons (see Fig 3F), cerebellum (see Fig 3H), including the number of Purkinje cells (wild type: 642 ± 6 cells/section; $ALS2^{-/-}$: 664 ± 62 cells/section; n = 3; $p = 0.74$, unpaired t test; see Fig 3I), primary motor cortex, and hippocampus (data not shown) even in the aged $ALS2^{-/-}$ mice.

Progressive Spinal Axon Degeneration in ALS2-Deficient and Mutant Superoxide Dismutase 1 Mice

A common clinical feature of *ALS2*-mutated patients both with the typical infantile onset (1–2 years old)[9–11,14,15,30] and the later juvenile onset[8] is progressive spasticity, suggesting a UMN defect (see the Table). In hereditary spastic paralysis that affects UMNs, a corticospinal tract (CST) lesion is the common pathological hallmark. To determine whether the impaired motor performance observed in $ALS2^{-/-}$ mice could be due to the degeneration of the CST, we examined cross sections of spinal cords from 16-month-old $ALS2^{-/-}$, normal littermate, and mutant $SOD1^{G85R}$ mice,[26] a mouse model for dominantly inherited ALS. In mice, most (80%) CST axons are located in the dorsal column (Fig 4A).[31,32] Surprisingly, almost all of these CST axons both from the cervical and lower thoracic cord were preserved in $ALS2^{-/-}$ mice. This was also true for $SOD1^{G85R}$ mice, in which few CST axons were degenerated even in end-stage animals (see Figs 4B–D and 5B). In contrast, swollen and degenerating axons were predominantly seen in the lateral column from $ALS2^{-/-}$ mice compared with wild-type mice (see Figs 4H, I). Counting of abnormal axons showed even more robust degeneration in lateral column axons in the end-stage $SOD1^{G85R}$ mice (see Figs 4J and 5A). Such axonal changes were not found in younger $ALS2^{-/-}$ or $SOD1^{G85R}$ mice (see Figs 4F, G). In mice, the lateral column contains descending axons including approximately 20% of CST axons (referred as dorsolateral CST),[32] rubrospinal tract, and tectospinal tract that contribute to motor control. In the lateral column of $ALS2^{-/-}$ mice, the distal axons in the lower thoracic cord were more affected than those in the cervical region (see Fig 5A), implicating retrograde axonal degeneration, as seen in human hereditary spastic paraplegia (HSP) patients.[33]

Discussion

Combined with the measurement of grip strength, we have demonstrated slowness of running speed without an effect on muscle weakness in $ALS2^{-/-}$ mice in an age-dependent manner. In human patients, including those with ALS, "slowness out of proportion to muscle weakness" is also recognized as a sensitive sign of a UMN defect.[23–25] Mice deficient for PLP (proteolipid protein)[27] and paraplegin,[28] which are mouse models for HSP, exhibit modest motor impairment similar to $ALS2^{-/-}$ mice.[22] Like the $ALS2^{-/-}$ mice, these models develop moderate declines of rotarod performance during aging; however, there has been no demonstration of a UMN defect in those mice. Indeed, little is known about UMN disease in rodents and the methods to analyze UMN defects. Here, we have established a simple method (running speed), which when combined with a measure of muscle strength may provide an assessment of UMN function. Although slowness without weakness could arise from a variety of causes including, for example, extrapyramidal disorders or joint disease, given the otherwise healthy condition of the $ALS2^{-/-}$ mice, the neuropathological findings in those mice, and the clinical deficit in human patients with *ALS2* mutations, we conclude that slowness without muscle weakness seen in $ALS2^{-/-}$ mice is due to a UMN defect. This phenotype contrasts with that of mutant SOD1 mice that develop severe lower motor neuron degeneration leading to prominent muscle weakness. Although not recognized in prior reports, this SOD1-mediated disease contains a UMN component, too, as demonstrated by obvious degeneration of the subset of UMN within the lateral spinal column.

In light of the typical infantile onset of severe spastic tetraplegia that is seen in *ALS2*-mutated patients, why was the UMN defect seen in the $ALS2^{-/-}$ mice so moderate? The motor impairment of $ALS2^{-/-}$ mice shown by us and others[21,22] was indeed mild. One possible explanation is the anatomical difference of UMN between human and rodents. The anatomy of CST of rodents differs markedly from humans in several ways. First, the majority of the CST descends in the ventromedial part of dorsal column in rodents (see Fig 4A), whereas it is located in the lateral column in human and nonhuman primates.[31,32] Second, although the dorsal column in human consists of ascending tract axons only, the dorsal column in rodents contains both CST and ascending sensory tracts (such as fasciculus gracilis). Third, the CST axons in rodents probably do not directly connect with spinal motor neurons but with interneurons, and corticomotor neuronal connections in

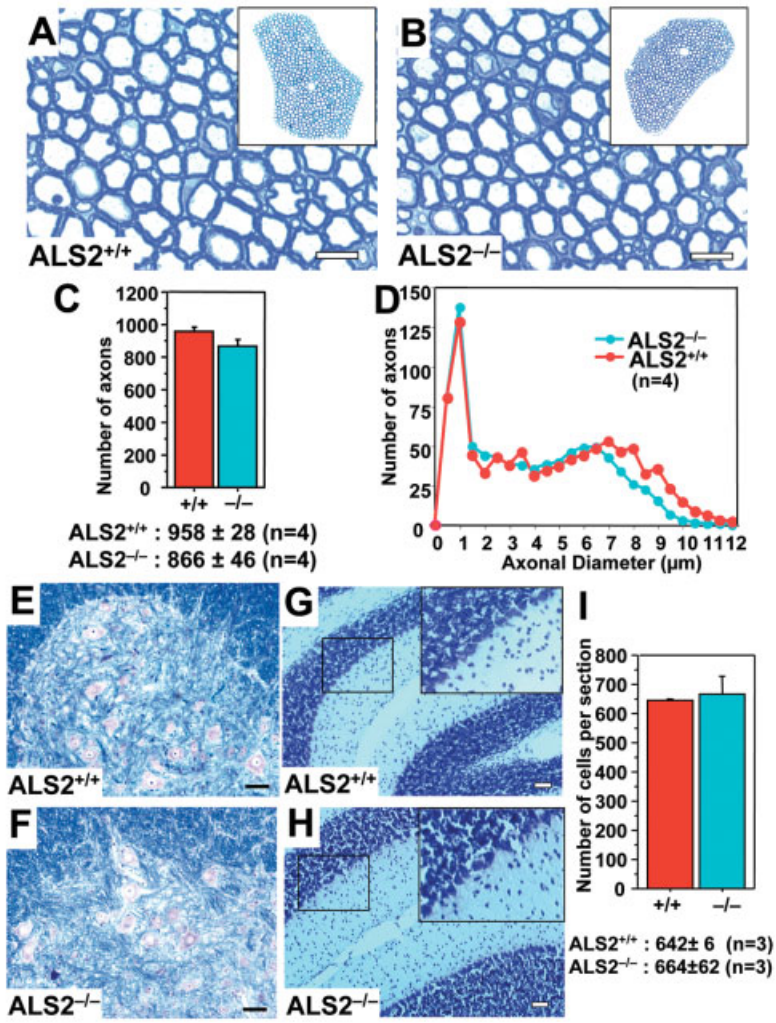

Fig 3. Lumbar motor neurons and cerebellum are preserved in ALS2$^{-/-}$ mice. (A, B) Cross sections of L5 motor roots from 16-month-old wild-type (A) and ALS2$^{-/-}$ (B) mice stained with toluidine blue. Insets show lower magnification. (C) Numbers of axons in L5 motor roots of 16-month-old wild-type (ALS2$^{+/+}$) and ALS2$^{-/-}$ mice. Counts are averages from four animals for each genotype. (D) Distributions of axonal diameters in motor axons in 16-month-old wild-type (ALS2$^{+/+}$) and ALS2$^{-/-}$ mice. Points represent the average distribution of axon diameters from the entire roots of four mice for each genotype. (E, F) Luxol fast blue staining of representative transverse sections of lumbar spinal cord from 16-month-old wild-type (E) and ALS2$^{-/-}$ mice (F). (G, H) Cresyl violet staining of representative sections of cerebellum from 16-month-old wild-type (G) and ALS2$^{-/-}$ mice (H). Insets show higher magnification of Purkinje cells. (I) Number of Purkinje cells per cerebellar sagittal section of 16-months-old wild-type (ALS2$^{+/+}$) and ALS2$^{-/-}$ mice. Counts are averages from three animals for each genotype. Bars = 10μm (A, B); 50μm (E–H).

rodents are thought to be exclusively polysynaptic.[31,34] Indeed, we have determined that the CST in the dorsal column was preserved in *ALS2*$^{-/-}$ mice and relatively preserved in an SOD1 mouse model, as is also the case for PLP$^{-/-}$ and paraplegin$^{-/-}$ mice.[27,28] The differences in UMN anatomy between rodents and human may explain moderate motor impairment and relative preservation of CST in the dorsal column seen in *ALS2*$^{-/-}$ mice relative to the much earlier onset and severity in humans. Added to this is the possibility of a more substantial contribution to ALS2 function in mice from the related ALS2-CL gene, which has a gene product that has a 50% similarity to the carboxyl-terminal portion of ALS2 including the vacuolar protein sorting 9 (VPS9) GEF domain and that can interact with Rab5 and modulate endosome dynamics.[35]

Despite Hadano and colleagues report[21] of decreased motor axons in 18-month-old *ALS2*$^{-/-}$ mice, neither we nor Cai and colleagues[22] observed any pathological changes in the lower motor neuron system. Moreover, in contrast with a reported loss of 22% of Purkinje cells in 18-month-old *ALS2*$^{-/-}$ mice,[21] careful examination of our *ALS2*$^{-/-}$ mice showed no losses or pathological changes in the cerebellum (see Figs 3H, I), the brain region where ALS2 protein accumulates to its highest level, but there was clear axonal degeneration in

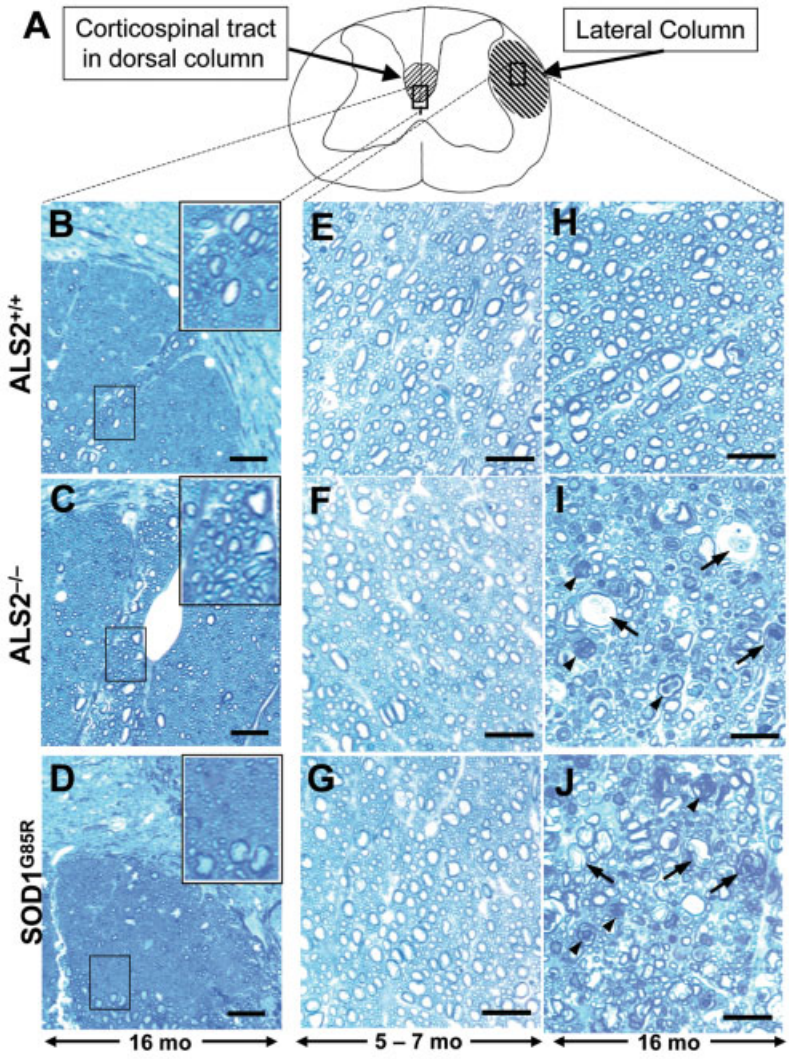

Fig 4. Progressive spinal axonal degeneration both in ALS2$^{-/-}$ and mutant superoxide dismutase 1 (SOD1) mice. (A) Schematic drawing of mouse spinal cord indicating corticospinal tract in dorsal column and lateral column shown in (B–J). (B–J) Representative toluidine blue staining of transverse sections of lower thoracic spinal cord from 16-month-old wild-type (B, H) and ALS2$^{-/-}$ (C, I) mice, and 12-month-old (end-stage) SOD1^{G85R} (D, J) mice. (B–D) Axons in the corticospinal tract in ventromedial part of dorsal column were preserved. Boxed areas *are magnified in the insets. (E–G) Normal structure of axons in lateral column in 7.5-month-old wild-type (E) and ALS2$^{-/-}$ (F) and 5-month-old SOD1^{G85R} mice (G). (H–J) Axonal degeneration in lateral column was seen in 16-month-old ALS2$^{-/-}$ mice (I), as well as end-stage SOD1^{G85R} mice (J), but not in wild-type mice (H). Representative degenerated axons are indicated with* arrows *(severely degenerated) and* arrowheads *(degenerated). Bars = 20μm.*

the lateral column of the spinal cord. The diversity of apparent phenotypes seen among the three independently produced *ALS2*$^{-/-}$ mice might be due to difference of genetic background or differences in the degree of gene inactivation from altered gene-targeting strategies. Although exon 4 was disrupted in our study, producing a predicted translation terminator at amino acid 175, exon 3 was disrupted by others, thereby producing a 14-amino acid predicted translation product. For each of these, it is hard to exclude the possible production of low levels of alternatively spliced variants that could provide some residual ALS2 function. Despite these differences, impaired rotarod performance was reported in all three *ALS2*$^{-/-}$ mice, albeit the result of Hadano and colleagues[21] did not reach statistical significance probably as a consequence of loss of sensitivity from a high accelerating rate of the rotating rod (80*g*/min) instead of 10*g*/min in this and Cai and colleagues' study.[22]

We have interpreted this impaired rotor-rod performance accompanied with slowness in motion as a UMN sign based on our pathological findings, although it is difficult to completely rule out the possibility of cerebellar or extrapyramidal contribution to this motor phenotype. In humans, the cerebellum is also known to contribute to muscle tone, because an

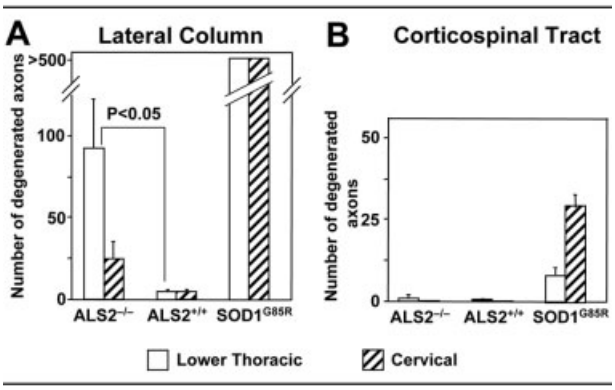

Fig 5. Quantification of axonal degeneration within spinal cords of $ALS2^{-/-}$ and $SOD1^{G85R}$ mice. (A, B) The lower thoracic spinal cord (open bar) *and cervical cord* (hatched bar) *sections from 16-month-old $ALS2^{+/+}$, $ALS2^{-/-}$, or 12-month-old $SOD1^{G85R}$ mice were analyzed. Average number of degenerated axons within lateral column (A) or corticospinal tract (B) from three mice per each genotype was shown. Statistical analysis was performed using unpaired* t *test.*

ablative lesion in the cerebellum typically causes a decrease in muscle tone.[23] Indeed, it is possible that part of the spasticity in ALS2 patients may be secondary to cerebellar deficits. Cerebellar dysfunction may be difficult to appreciate in these patients because the severe spasticity may mask other clinical signs including the expected ataxia. Future autopsy studies of patients may uncover cerebellar involvement in this disease.

The progressive axonal degeneration in aged $ALS2^{-/-}$ mice provides evidence that ALS2 does play a role in maintenance of a subset of spinal cord axons, those in the dorsolateral CST, which may have a direct connection with spinal motor neurons.[32] The dorsolateral CST, as well as many descending tracts that participate in motor control such as rubrospinal and tectospinal tracts, are located in the lateral column. Degeneration of these axons was seen in both $ALS2^{-/-}$ and mutant SOD1 mouse models, demonstrating vulnerability of these axons in those models. Moreover, a gradient of an increased number of degenerated axons in lower thoracic cord versus cervical cord raises the possibility of retrograde axonal degeneration of descending axons (see Fig 5A), a finding consistent with ascending disease progression from lower to the upper limbs seen in patients with *ALS2* mutations.[9,30] Although tracer-mediated visualization of such tracts may be challenging due to a transport defect(s) expected in degenerating axons, an effort to identify the origin of these degenerating tracts in mouse models may provide a mechanistic view of UMN degeneration. The proposed role of ALS2 in vesicular trafficking[17] and/or neurite extension[20] through Rab5 and/or Rac1 GEF activities, respectively, might explain the spinal axonal degeneration of $ALS2^{-/-}$ mice seen in this study, although these hypotheses have been tested only with $ALS2^{-/-}$ fibroblasts, in which altered endosome trafficking has been reported.[21]

Finally, $ALS2^{-/-}$ mice generated in this study exhibit a moderate, age-dependent impairment of motor coordination and slowness of movement likely due to the progressive spinal axonal degeneration with preservation of lower motor neurons, consistent with HSP mouse models. Our study, together with clinical reports of patients with *ALS2* mutations,[30] illustrates that ALS2 is a severe UMN disease that closely resembles HSP, but is quite distinct from sporadic or familial ALS. Future elucidation of the physiological role of ALS2 in neuronal maintenance will provide further understanding of the mechanism underlying UMN degeneration.

This work was supported by a Research fellowship from Uehara Memorial Foundation, the Muscular Dystrophy Association (Developmental Grant, K.Y.), the NIH (K12 Grant, AG000975-04, T.M.M.; NS27036, D.W.C.), and the Packard ALS Center at Johns Hopkins (D.W.C.). D.W.C. receives salary support from Ludwig Institute for Cancer Research.

We thank Drs P. Leder and A. Wynshaw-Boris for TC1 cells, Dr C. Vande Velde for antibody preparation, Dr Y. Wang for embryonic stem cell culture, and J. Folmer and M. A. Lawrence for expert assistance with tissue preparation.

References

1. Cleveland DW, Rothstein JD. From Charcot to Lou Gehrig: deciphering selective motor neuron death in ALS. Nat Rev Neurosci 2001;2:806–819.
2. Bruijn LI, Miller TM, Cleveland DW. Unraveling the mechanisms involved in motor neuron degeneration in ALS. Annu Rev Neurosci 2004;27:723–749.
3. Hentati A, Bejaoui K, Pericak-Vance MA, et al. Linkage of recessive familial amyotrophic lateral sclerosis to chromosome 2q33–q35. Nat Genet 1994;7:425–428.
4. Hosler BA, Sapp PC, Berger R, et al. Refined mapping and characterization of the recessive familial amyotrophic lateral sclerosis locus (ALS2) on chromosome 2q33. Neurogenetics 1998;2:34–42.
5. Hadano S, Nichol K, Brinkman RR, et al. A yeast artificial chromosome-based physical map of the juvenile amyotrophic lateral sclerosis (ALS2) critical region on human chromosome 2q33–q34. Genomics 1999;55:106–112.
6. Hadano S, Hand CK, Osuga H, et al. A gene encoding a putative GTPase regulator is mutated in familial amyotrophic lateral sclerosis 2. Nat Genet 2001;29:166–173.
7. Yang Y, Hentati A, Deng HX, et al. The gene encoding alsin, a protein with three guanine-nucleotide exchange factor domains, is mutated in a form of recessive amyotrophic lateral sclerosis. Nat Genet 2001;29:160–165.
8. Ben Hamida M, Hentati F, Ben Hamida C. Hereditary motor system diseases (chronic juvenile amyotrophic lateral sclerosis). Conditions combining a bilateral pyramidal syndrome with limb and bulbar amyotrophy. Brain 1990;113(pt 2):347–363.
9. Eymard-Pierre E, Lesca G, Dollet S, et al. Infantile-onset ascending hereditary spastic paralysis is associated with mutations in the alsin gene. Am J Hum Genet 2002;71:518–527.
10. Gros-Louis F, Meijer IA, Hand CK, et al. An ALS2 gene mutation causes hereditary spastic paraplegia in a Pakistani kindred. Ann Neurol 2003;53:144–145.

11. Devon R, Helm J, Rouleau G, et al. The first nonsense mutation in alsin results in a homogeneous phenotype of infantile-onset ascending spastic paralysis with bulbar involvement in two siblings. Clin Genet 2003;64:210–215.
12. Lerman-Sagie T, Filiano J, Smith DW, Korson M. Infantile onset of hereditary ascending spastic paralysis with bulbar involvement. J Child Neurol 1996;11:54–57.
13. Gascon GG, Chavis P, Yaghmour A, et al. Familial childhood primary lateral sclerosis with associated gaze paresis. Neuropediatrics 1995;26:313–319.
14. Kress JA, Kuhnlein P, Winter P, et al. Novel mutation in the ALS2 gene in juvenile amyotrophic lateral sclerosis. Ann Neurol 2005;58:800–803.
15. Eymard-Pierre E, Yamanaka K, Haeussler M, et al. Novel missense mutation in ALS2 gene results in IAHSP. Ann Neurol 2006;59:976–980.
16. Yamanaka K, Vande Velde C, Eymard-Pierre E, et al. Unstable mutants in the peripheral endosomal membrane component ALS2 cause early-onset motor neuron disease. Proc Natl Acad Sci U S A 2003;100:16041–16046.
17. Otomo A, Hadano S, Okada T, et al. ALS2, a novel guanine nucleotide exchange factor for the small GTPase Rab5, is implicated in endosomal dynamics. Hum Mol Genet 2003;12: 1671–1687.
18. Topp JD, Gray NW, Gerard RD, Horazdovsky BF. Alsin is a Rab5 and Rac1 guanine nucleotide exchange factor. J Biol Chem 2004;279:24612–24623.
19. Kanekura K, Hashimoto Y, Kita Y, et al. A Rac1/phosphatidylinositol 3-kinase/Akt3 anti-apoptotic pathway, triggered by AlsinLF, the product of the ALS2 gene, antagonizes Cu/Zn-superoxide dismutase (SOD1) mutant-induced motoneuronal cell death. J Biol Chem 2005;280:4532–4543.
20. Tudor EL, Perkinton MS, Schmidt A, et al. ALS2/Alsin regulates Rac-PAK signaling and neurite outgrowth. J Biol Chem 2005;280:34735–34740.
21. Hadano S, Benn SC, Kakuta S, et al. Mice deficient in the Rab5 guanine nucleotide exchange factor ALS2/alsin exhibit age-dependent neurological deficits and altered endosome trafficking. Hum Mol Genet 2006;15:233–250.
22. Cai H, Lin X, Xie C, et al. Loss of ALS2 function is insufficient to trigger motor neuron degeneration in knock-out mice but predisposes neurons to oxidative stress. J Neurosci 2005;25: 7567–7574.
23. Merritt HH, Rowland LP. Merritt's textbook of neurology. 10th ed. Philadelphia: Lippincott Williams & Wilkins, 2000.
24. Bradley WG. Neurology in clinical practice. 4th ed. Philadelphia: Butterworth-Heinemann, 2004.
25. Braunwald E. Harrison's principles of internal medicine. 15th ed. New York: McGraw-Hill, 2001.
26. Bruijn LI, Becher MW, Lee MK, et al. ALS-linked SOD1 mutant G85R mediates damage to astrocytes and promotes rapidly progressive disease with SOD1-containing inclusions. Neuron 1997;18:327–338.
27. Griffiths I, Klugmann M, Anderson T, et al. Axonal swellings and degeneration in mice lacking the major proteolipid of myelin. Science 1998;280:1610–1613.
28. Ferreirinha F, Quattrini A, Pirozzi M, et al. Axonal degeneration in paraplegin-deficient mice is associated with abnormal mitochondria and impairment of axonal transport. J Clin Invest 2004;113:231–242.
29. Zanjani H, Lemaigre-Dubreuil Y, Tillakaratne NJ, et al. Cerebellar Purkinje cell loss in aging Hu-Bcl-2 transgenic mice. J Comp Neurol 2004;475:481–492.
30. Lesca G, Eymard-Pierre E, Santorelli FM, et al. Infantile ascending hereditary spastic paralysis (IAHSP): clinical features in 11 families. Neurology 2003;60:674–682.
31. Terashima T. Anatomy, development and lesion-induced plasticity of rodent corticospinal tract. Neurosci Res 1995;22: 139–161.
32. Steward O, Zheng B, Ho C, et al. The dorsolateral corticospinal tract in mice: an alternative route for corticospinal input to caudal segments following dorsal column lesions. J Comp Neurol 2004;472:463–477.
33. Reid E. The hereditary spastic paraplegias. J Neurol 1999;246: 995–1003.
34. Yang HW, Lemon RN. An electron microscopic examination of the corticospinal projection to the cervical spinal cord in the rat: lack of evidence for cortico-motoneuronal synapses. Exp Brain Res 2003;149:458–469.
35. Hadano S, Otomo A, Suzuki-Utsunomiya K, et al. ALS2CL, the novel protein highly homologous to the carboxy-terminal half of ALS2, binds to Rab5 and modulates endosome dynamics. FEBS Lett 2004;575:64–70.